Desalination and Water Treatment
www.deswater.com

doi: 10.1080/19443994.2016.1143881

57 (2016) 25080–25088
November

Taylor & Francis
Taylor & Francis Group

Adsorption behaviour of copper onto a novel modified chitosan material: thermodynamic study

N. Flores-Alamo[a,b,c], R.M. Gómez-Espinosa[b], M. Solache-Ríos[a,*], J.L. García-Rivas[c], R.E. Zavala-Arce[c], B. García-Gaitán[c]

[a] *Departamento de Química, Instituto Nacional de Investigaciones Nucleares, D.F., C.P. 11801, Apdo, Postal 18-1027, Mexico, email: alamofn@gmail.com (N. Flores-Alamo), Tel. +52 5553297200; Fax: +52 5553297301; email: marcos.solache@inin.gob.mx (M. Solache-Ríos)*

[b] *Facultad de Química, Universidad Autónoma del Estado de México, Paseo Colón y Tollocan S/N., Toluca, Estado de México, C.P. 50000, Mexico, email: rosamarigo@gmail.com (R.M. Gómez-Espinosa)*

[c] *División de estudios de Posgrado e Investigación, Instituto Tecnológico de Toluca, Av. Instituto Tecnológico S/N, Fracc. La Virgen Metepec, Estado de México, C.P. 52140, Mexico, emails: lgrivas230@yahoo.com.mx (J.L. García-Rivas), zavalaarce@yahoo.com (R.E. Zavala-Arce), beatrizggmx@yahoo.com (B. García-Gaitán)*

Received 13 August 2015; Accepted 12 January 2016

ABSTRACT

The adsorption behaviour of Cu(II) was investigated in the presence of a new material. This material was obtained from chitosan (Ch) and polyvinyl alcohol (PVA) at different weight percentages (35/65, 50/50 and 65/35), dripping this mixture in a NaOH solution, and then subjecting to crosslinking reaction under nitrogen atmosphere at 353 K with ethylene glycol diglycidyl ether to improve its resistance to acids and alkalis. Adsorption test were conducted to evaluate the optimal Ch/PVA ratio, 35/65 ratio presented the best adsorption capacity. The interaction between Cu(II) and functional groups of Ch/PVA was determined by Fourier transformed infrared spectroscopy. Kinetics and isotherm experiments were performed to evaluate the adsorption behaviour of Cu(II). The kinetic experimental data were best fitted to pseudo-second-order model and equilibrium data to the Langmuir model. Thermodynamics parameters such as free Gibbs energy (ΔG°), enthalpy (ΔH°) and entropy (ΔS°) were calculated. These parameters indicated spontaneous and endothermic adsorption process.

Keywords: Adsorption; Thermodynamic parameters; Crosslinked chitosan; Copper

1. Introduction

The adsorption process has been widely studied as an alternative method to remove heavy metals present in water as the result of industrial effluents that endangers the environment [1,2]. Metallurgy industries release huge amounts of heavy metals such as copper, which is toxic due to its non-biodegradable and carcinogenic nature [1–4].

Thermodynamic parameters can be evaluated by kinetics adsorption studies. Equilibrium adsorption is reached when the adsorbate concentration in the solution is in dynamic balance with the adsorbent. This equilibrium can be described by some adsorption isotherms, such as Langmuir and Freundlich [5–8].

---

*Corresponding author.

The adsorption rate of the metallic ions by an adsorbent is determined by the adsorption kinetic, models such as pseudo-first-order (Langergren) or pseudo-second-order (Ho and McKay) have been used to treat the experimental data in order to determine the behaviour of the adsorption processes [8–13].

Recently, one of the bio-based materials used as an adsorbent for heavy metals is chitosan, because it is abundant in nature [14–16]. Chitosan (Ch) or poly(β-1–4)-2-amino-2-deoxy-D-glucopyranose, is obtained from the alkaline deacetylation of chitin. This material exhibits a great affinity for transition metals because the amino (–NH_2) and hydroxyl (–OH) groups of the chitosan chain are the coordination sites [17–20]. One of the polymers used to modify the mechanic and thermal resistance of chitosan is polyvinyl alcohol (PVA) [17,21]. Crosslinking is also a good option to improve the resistance of the material; some of the most used crosslinkers are ethylene glycol diglycidyl ether (EGDE), epichlorohydrin and glutaraldehyde [17,21–23].

In this work, the kinetic, thermodynamic parameters and equilibrium isotherm were determined in order to elucidate the adsorption mechanism of copper by a new material synthesized from Ch and PVA crosslinked with EGDE.

2. Materials and methods

2.1. Materials

Chitosan industrial grade with a 65% of deacetylation from Química América, high density PVA 99% hydrolysed from Golden Bell and EGDE at 50% from Sigma Aldrich were used to synthesize the adsorbent material. Aqueous solutions were prepared using anhydrous copper sulphate, glacial acetic acid at 99%. Deionized water was used in all experiments.

2.2. Synthesis of the adsorbent material

Adsorbent material beads were synthesized from Ch and PVA, crosslinked with EGDE (Ch/PVA/EGDE). Beads were prepared with three different Ch/PVA ratios. Chitosan hydrogel beads were prepared using a phase inversion technique [20], weighing 3.1, 3.25 and 3.8 g of Ch and dissolving in a 0.4 M acetic acid solution at 298 K and then these solutions were stirred for 12 h at 500 rpm. PVA was dissolved in DI water (7.7%) at 343 K and stirred at 500 rpm for 2 h. The solutions of Ch and PVA were mixed and stirred at 400 rpm to obtain Ch/PVA ratios of 35/65, 50/50 and 65/35 weight per cent. Each mixture was dripped in a 1 M sodium hydroxide solution stirring at 200 rpm using a 9-mm diameter needle. Crosslinking reaction was performed with a solution of EGDE, initial pH of 12, under nitrogen atmosphere with continuous stirring at 353 K in a water bath for 6 h. Ch/PVA beads/EGDE ratio was 7 mL/0.1 g for each 25 mL of deionized water. Finally, the beads were separated from the NaOH solution and washed with deionized water until the pH of solution was the same as that of deionized water, and stored in deionized water.

2.3. Characterization of the Ch/PVA/EGDE beads

Adsorbent material was analysed before and after Cu(II) adsorption by low vacuum scanning electron microscope (SEM) coupled with energy-dispersive X-ray analysis (EDS) (JEOL JSEM-590-LD) in order to determine the percentages of C, O, N and Cu present in both, external (E.S.) and internal (I.S.) surfaces of the Ch/PVA/EGDE beads, the analysis was performed in five different sites at 20 kV.

Infrared spectroscopy analysis (Fourier transformed infrared spectroscopy (FTIR)) was performed to determine functional groups present in Ch/PVA/EGDE beads and Cu(II) saturated material. Infrared spectra were obtained using a Bruker Tensor27 spectrometer with Platinum ATR accessory, 32 scans at a resolution of 1 cm^{-1} were averaged. Resonance Raman spectra were obtained with a LabRam HR 800 Jobin Yvon. Excitation laser was provided at 532 nm with a power ca. 70 mW at the sample. The slit width was 600 mm^{-1}, and the acquisition time for each scan was 10 s with 50 drifts.

Zero point charge (pHZPC) was performed as follows: experiments were accomplished in aqueous solutions varying initial pH (pH_{ini}) from 3 to 10, initial pH values were adjusted using either 0.1 M HNO_3 or 0.1 M NaOH solutions. Amounts of 0.5 g of wet Ch/PVA/EGDE beads and 20-mL aliquots of $NaNO_3$ solution (0.1 M) were stirred for 24 h at 298 K. Then the pH of each solution (pH_{eq}) was measured and pHZPC was determined by the intersection of the curve to *Y*-axis of a plot ΔpH ($pH_{ini} - pH_{eq}$) vs. pH_{ini} [24–26].

2.4. Ch/PVA/EGDE stability in acid solutions

Degradation behaviour of the material was investigated by weight loss measurements. The weight loss of the material was determined after the material was in contact with acid solutions (HCl, HNO_3, H_2SO_4 and $C_4H_4O_2$) of pH 1, 2 and 4. 0.5 g of sample beads were put in contact with 20 mL of each acid solution; the samples were shaken for 48 h at 298 K. After 48 h, the phases were separated (by filtration) and the solids were weighed.

2.5. Batch adsorption experiments

All the experiments that involved adsorption of Cu(II) in aqueous solutions were conducted by triplicate using wet beads, and were maintained under continuous shaking using a Heidolph thermal mixer at 200 rpm. Cu(II) concentrations were measured using a GB-932 plus atomic absorption spectrophotometer (AAS) at λ = 327.4 nm.

2.5.1. Effect of Ch/PVA ratio

Batch adsorption experiments were carried out using the synthesized material (Ch/PVA/EGDE) with different Ch/PVA ratios (35/65 50/50 y 65/35 wt.%). Amounts of 0.5 g of wet beads (corresponding to 0.005 g of dry beds) and 20 mL of 20 mg/L of a Cu(II) solution at initial pH of 5 were stirred at 298 K for 24 and 48 h. Cu(II) concentrations were measured and the capacities of adsorption at equilibrium (q_e) were calculated using Eq. (1):

$$q_e = \frac{(C_0 - C_e) \cdot V}{w} \tag{1}$$

where C_0 and C_e are the initial and equilibrium (final) Cu(II) concentration (mg/L), respectively, V is the solution volume (L) and w is the weight of dried Ch/PVA/EGDE (g).

2.5.2. pH effect on adsorption capacity

Adsorption behaviour tests at different pH values were carried out placing 0.5 g of wet adsorbent in 20 mL of 20 mg/L Cu(II) solution at 298 K at different initial pH from 1 to 7 and they were stirred for 24 h. The pH was adjusted using HNO_3 or NaOH solutions and it was measured using an Orion 3-Star plus pH meter and then Cu(II) concentrations were determined as described above.

2.5.3. Kinetic experiments and thermodynamic parameters

Kinetic experiments were performed at 298, 308, 318 and 328 K. 0.5 g of wet Ch/PVA/EGDE beads (corresponding to 0.005 g of dry beds) were left in contact with 20 mL of Cu(II) with an initial concentration of 20 mg/L and initial pH of 5. The samples were stirred during 0.25, 0.5, 0.75, 1, 2, 3, 4, 5, 6, 8, 12, 18, 24, 36 and 48 h. The concentrations of Cu(II) ions were measured and adsorption capacities were calculated considering the weight corresponding to dry material.

Experimental data were fitted to pseudo-first-order [2] and pseudo-second-order [9, 10] models, using the software Origin 8.1. The pseudo-first-order model is represented in Eq. (2):

$$q_t = q_e(1 - e^{-k_1 t}) \tag{2}$$

where q_e and q_t are the capacities of adsorption at equilibrium and at any time t (mg/g), k_1 is the rate constant of first-order adsorption (1/min).

The pseudo-second-order model is represented in Eq. (3):

$$q_t = \frac{k_2 q_e^2 t}{1 + k_2 q_e t} \tag{3}$$

where k_2 is the rate constant of the pseudo-second-order equation (g/mg min).

Thermodynamic parameters: enthalpy (ΔH°), entropy (ΔS°) and Gibbs free energy (ΔG°) were calculated using the results of the adsorption equilibrium determined at different temperatures, Van't Hoff equation was used for calculations:

$$\ln(K_c) = \frac{\Delta S^\circ}{R} - \frac{\Delta H^\circ}{R} \cdot \left(\frac{1}{T}\right) \tag{4}$$

$$\Delta G^\circ = \Delta H^\circ - T \cdot \Delta S^\circ \tag{5}$$

where $K_c = q_e/C_e$, R is the universal gas constant (kJ/mol K) and T is the temperature (K).

2.5.4. Adsorption isotherm

The adsorption isotherm was carried out using 20 mL of Cu(II) solutions (concentrations from 2 to 50 mg/L); each solution was left in contact with 0.5 g of wet Ch/PVA/EGDE beads. Initial pH was adjusted to 5 and samples were stirred at 298 K for 48 h. Cu(II) ion concentrations were measured and the equilibrium data were treated with the Langmuir and the Freundlich nonlinear adsorption isotherms.

Eq. (6) represents the Langmuir isotherm, which is valid for monolayer adsorption onto a surface with a finite number of identical sites [8,14]:

$$q_e = \frac{q_{\max} b C_e}{1 + b C_e} \tag{6}$$

where $q_{\max}$ is the maximum adsorption at monolayer (mg/g), and b is the Langmuir constant related to the affinity of binding sites (mL/mg).

Eq. (7) represents the empirical Freundlich isotherm based on adsorption on heterogeneous surface [8,14]:

$$q_e = K_F\, C_e^{1/n} \tag{7}$$

where K_F and n are the Freundlich constants indicating sorption capacity (mg/g) and intensity, respectively.

2.6. Adsorption–desorption cycles

Batch experiments were performed using three regenerating agents, HCl, HNO_3 and EDTA solutions of pH 2, 3 and 4. 0.5 g of Ch/PVA/EGDE was treated with a 50 mg/L Cu(II) solution. The resulting samples were treated with 20 mL of each agent solution for 0.5, 1, 3 and 10 h. Adsorption–desorption cycles were performed three times, maintaining the same experimental conditions. After each desorption process, beds were separated from each regenerating agent, washed with 20 mL of deionized water and then fresh solution of Cu(II) (pH 5) was added. The concentration of copper was measured before and after each adsorption–desorption cycle.

3. Results and discussion

3.1. Scanning electron microscopy

Fig. 1(a) and (b) shows the morphology of Ch/PVA/EDGE beads, their average size is 2.1 ± 0.11 mm. The high porosity of the material can be observed in Fig. 1(b). The pore diameter ranged from 11 to 79 μm, which is favourable for the metallic ions to enter into the adsorbent material beads.

Table 1 summarizes the results of the elemental analysis (EDS) of beads before and after adsorption.

The presence of sulphur could be attributed to copper sulphate used to prepare the solutions of Cu(II). Table 1 shows presence of Cu(II) adsorbed onto external (E.S.) and internal surface (I.S), it is clear that Cu(II) is mainly retained on the external surface.

3.2. FTIR-ATR analysis

FTIR analysis of Ch/PVA/EGDE beads was performed in order to identify the functional groups that may interact with Cu(II) ions. The spectra of Ch/PVA/EGDE before adsorption, show bands at 3,353–3,301 cm^{-1} corresponding to primary amine ($–NH_2$) and –OH groups. The N–H vibration of chitosan is observed, at 1,590 cm^{-1} (Fig. 2). The analysis of FTIR data showed that each particular polysaccharide has a specific band in 1,200–1,000 cm^{-1} region [27]. This region is dominated by ring vibrations overlapped with stretching vibrations of (C–OH) side groups and the (C–O–C) glycosidic bond vibration, these bonds are found at 1,066 and 1,026 cm^{-1}. Ch/PVA/EGDE-Cu spectrum shows some changes after adsorptions in some specific groups. The region corresponding to $–NH_2$ and –OH shows a very wide band at 3,239 cm^{-1}, which indicates that, the amine and hydroxyl groups are involved in the coordination of Cu ions. Besides, the band at 1,590 cm^{-1} is shifted to 1,605 cm^{-1} due to coordination of –NH with Cu(II). The 1,066–1,026 cm^{-1} bands are shifted to 1,054 cm^{-1} indicating the same behaviour. These show that both peaks are involved in the interaction of NH_2 and OH groups with Cu(II) [28–32].

3.3. RAMAN analysis

Raman spectra are reported in order to analyse the Cu–N stretching vibrations, the Raman intensity of Cu–N vibration was found at 473 cm^{-1} (Fig. 3), characteristic of Cu–N stretching vibration [32,33].

3.4. Zero point charge

Fig. 4 shows the plot of ΔpH vs. pH_{ini}. The pH of pHZPC for Ch/PVA/EGDE was 7.5. This implies that at this pH, the net charge of the surface is zero. Above this pH, the net charge is negative as the result of the deprotonation of the amine groups. For a pH below the pHZPC, a net positive charge prevails due to the protonation of NH_2 groups of chitosan [8,23–25].

3.5. Ch/PVA/EGDE stability in acid solutions

The material was not stable at low pH acid solutions (Table 2); at pH 1 there was a relatively high weight loss after each acid treatment. $C_2H_4O_2$ and HNO_3 were the most aggressive acids to the sample because the weight losses were 74 and 48%, respectively. Furthermore, there was also fragmentation of the material at pH 1, perhaps due to the incompatibility of crosslinking (EGDE) to acids. The material showed good stability at pH 4; therefore, all experiments were performed at pH ≥ 5.

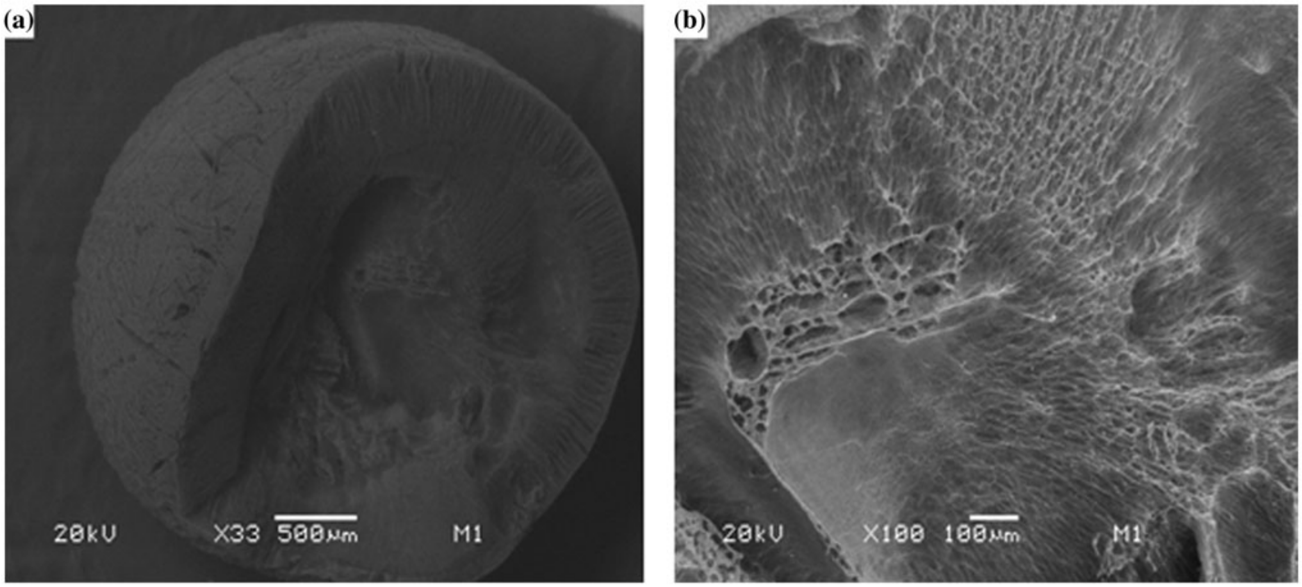

Fig. 1. SEM images showing the surface morphologies of Ch/PVA/EDGE beads.

Table 1
Elemental analysis of Ch/PVA/EGDE beads

Element	Material composition before adsorption of Cu(II)		Material composition after adsorption of Cu(II)	
	E.S. (%)	I.S. (%)	E.S. (%)	I.S. (%)
C	41.5 ± 3.1	46.8 ± 0.2	46.9 ± 3.5	45.7 ± 0.4
N	15.7 ± 8.4	10.0 ± 1.2	12.0 ± 3.9	9.7 ± 2.7
O	42.8 ± 5.5	43.2 ± 1.2	32.7 ± 8.4	43.0 ± 2.7
S	–	–	2.3 ± 0.9	0.8 ± 0.1
Cu	–	–	6.1 ± 3.4	0.8 ± 0.3

Notes: E.S.: External surface.
I.S.: Internal surface.

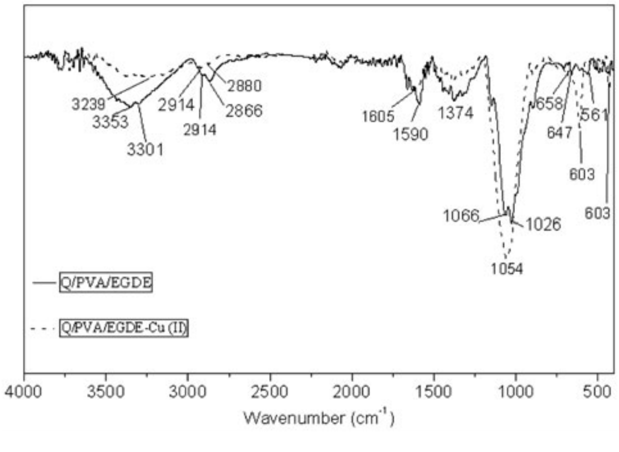

Fig. 2. FTIR spectra of Ch/PVA/EGDE and Ch/PVA/EGDE–Cu(II) beads.

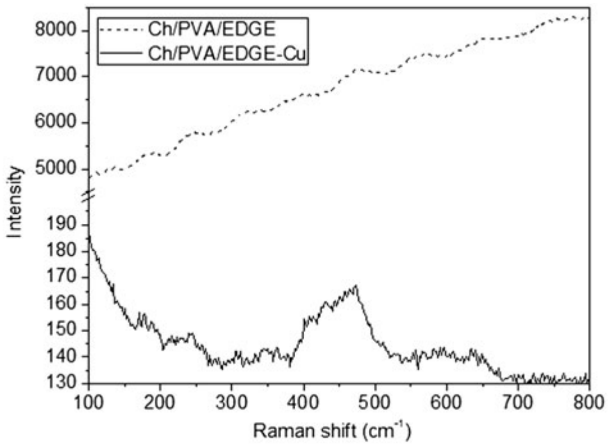

Fig. 3. Raman spectra of Ch/PVA/EGDE–Cu(II).

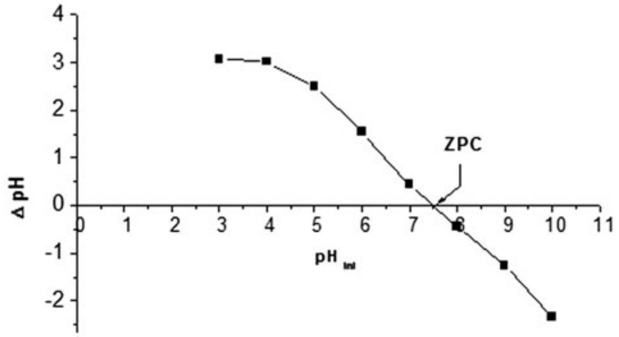

Fig. 4. ΔpH vs. pH_{ini} ZPC.

Table 2
Stability of Ch/PVA/EGDE in acid solutions

Acid	pH	% of weight lost	Appearance	Fragmentation
HCl	1	36	White	✓
	2	3	White	
	4	0	White	
HNO_3	1	48	White	✓
	2	8	White	
	4	0	White	
H_2SO_4	1	20	White	✓
	2	3	Pale	✓
	4	0	White	
$C_2H_4O_2$	1	74	White	✓
	2	0	White	
	4	0	White	

3.6. Adsorption of Cu(II) ions in an aqueous solution

3.6.1. Influence of the Ch/PVA ratio on the adsorption capacity

The adsorption capacities of Ch/PVA (35/65, 50/50 and 65/35 wt %) ratios for Cu(II) at equilibrium in an aqueous solution were 78.35 ± 0.36, 78.08 ± 0.33 and 77.48 ± 0.57 mg/g, respectively, for a contact time of 24 h, and values of 78.83 ± 0.36, 77.91 ± 0.18 and 78.31 ± 0.21 mg/g for 48 h. It is observed that the Ch/PVA ratios for Cu(II) adsorption were similar, it is important to note that Ch is more expensive than PVA, so it is advisable to use the 35/65 ratio without compromising the ability to remove heavy metals.

3.6.2. Effect of pH on the adsorption capacity of Cu(II)

The effects of pH values on metal uptake capacities are shown in Fig. 5. It is observed that the maximum adsorption capacity (q_e) of Cu(II) ions was 76.8 mg/g at initial pH of 5.

The uptake of Cu(II) increased suddenly from pH of 3 to 3.5 and the optimal pH for metal adsorption was 5. Chen et al. [23] and Ngah et al. [8] reported the adsorption capacities of Cu(II) by chitosan crosslinked with glutaraldehyde and non-crosslinked Ch/PVA at different pH values, the capacities were low at low pH values as observed in this work, they reported that the formation of $–NH^{3+}$ ions was responsible for this behaviour.

3.6.3. Adsorption kinetics

The effect of temperature on the adsorption of Cu(II) by Ch/PVA/EGDE at 298, 308, 318 and 328 K is shown in Fig. 6. Increasing the temperature does not significantly improve the adsorption capacity of the material. The adsorption rate was fast within the period from 0 to 2.5 h, after this time, the adsorption rate decreased up to the equilibrium and reached in around 12 h. The pH values at equilibrium were from 6.2 to 6.5. The adsorption rates for the different temperatures were similar as observed in Table 2 (k_2 values).

Adsorption kinetics data were examined using pseudo-first and pseudo-second-order models, the parameters determined by these models are given in Table 3 at different temperatures.

The data were adjusted to both models; q_e values were similar to q_{exp} value and R^2 were similar for both models. The first one indicates physical adsorption and the second chemical adsorption; in this last case, the rate-limiting step is attributed to chemical adsorption and the mechanism may involve valence forces in which the electrons are shared between metal and the

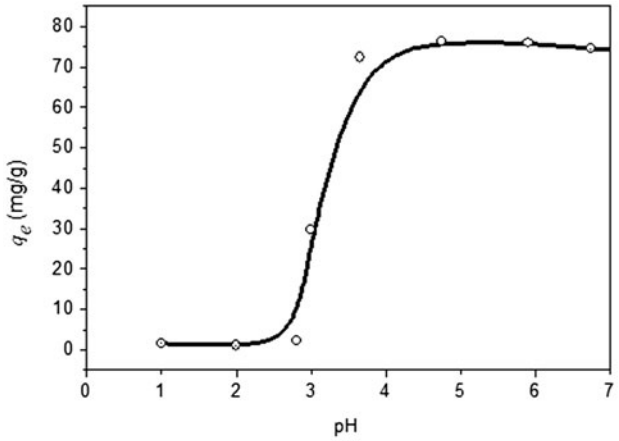

Fig. 5. Effect of pH on the adsorption capacity of Cu(II).

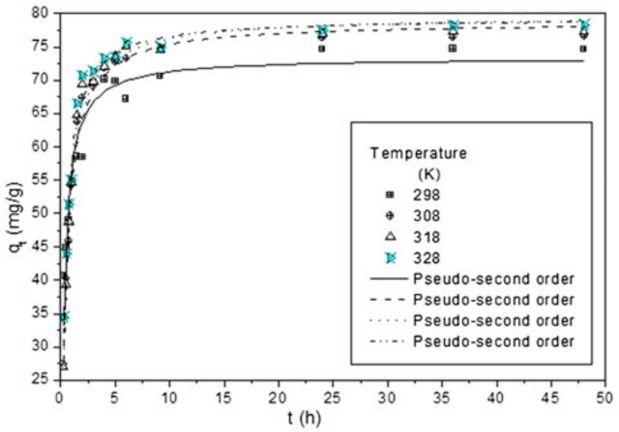

Fig. 6. Adsorption kinetic~~s~~ data fitted to pseudo-second-order model.

adsorbent [9]. According to the thermodynamic parameters obtained, physical adsorption is the most probable mechanism involved in this process as discussed in Section 3.6.4.

Chemical adsorption has been reported for the adsorption of Cu(II) by chitosan crosslinked with epichlorohydrin [23], and non-crosslinked chitosan/PVA [4,7,8,33].

3.6.4. Adsorption thermodynamics

The thermodynamic parameters ΔH° and ΔS° were determined using the Van't Hoff equation (Eq. (4)), and results are presented on Table 4. These parameters indicate that the nature of adsorption process is spontaneous since ΔG° was negative for all temperatures under study. The positive ΔH° confirms that the process was endothermic and the low positive value of ΔS° suggests a reversible adsorption [5,6,33].

Table 4
Thermodynamic parameters for Cu(II) adsorption

Temperature (K)	ΔG° (kJ/mol)	ΔH° (kJ/mol)	ΔS° (kJ/mol)
298	–19.7 ± 0.1	28.6 ± 1.8	0.16 ± 0.006
308	–21.4 ± 0.1		
318	–23.0 ± 0.1		
328	–24.6 ± 0.2		

Wang et al. [34], reported that physisorption commonly occurs when enthalpies are below 40 kJ/mol; according to the results, physisorption is the predominant adsorption process. Moreover, the positive value of enthalpy shows that the adsorption process is endothermic and the negative trend of ΔG is representative of a spontaneous process [4]. These results are similar to those reported by Kamari and Ngah, [22], they found negative values for ΔG and a ΔH of 31.5 kJ/mol using chitosan modified with H_2SO_4.

3.6.5. Adsorption equilibrium isotherm

Fig. 7 shows the equilibrium curve for different concentrations of Cu(II) ions in aqueous solutions in contact with Ch/PVA/EGDE at 298 K. The experimental data were treated with the Langmuir and Freundlich models; however, the data were best fitted to the Langmuir model (Table 5), which indicates that Ch/PVA/EGDE is a homogeneous adsorbent material. The pH equilibrium was between 6.8 and 7.1.

The results obtained for the adsorption equilibrium are similar to those reported by Chen et al. [23], Ngah et al. [21] and Dalida et al. [33]. Volesky and Holan [35] observed that the isotherms could hardly have a meaningful physical interpretation in biosorption.

Table 3
Kinetic parameters for Cu(II) adsorption

	T (K)			
Model	298	308	318	328
Pseudo-first-order				
q_e (mg/g)	69.2 ± 2.0	73.7 ± 0.9	74.5 ± 0.8	74.7 ± 1.2
$k_1 \times 10^{-2}$ (1/h)	3.3 ± 0.5	2.5 ± 0.1	2.4 ± 0.1	2.8 ± 0.2
R^2	0.91	0.99	0.98	0.97
Pseudo-second-order				
q_e (mg/g)	73.4 ± 1.4	78.7 ± 0.8	79.6 ± 0.9	79.3 ± 0.8
$k_2 \times 10^{-4}$ (g/mg h)	7.5 ± 1.0	4.7 ± 0.2	4.7 ± 0.3	5.7 ± 0.3
R^2	0.95	0.99	0.98	0.98
q_{exp} (mg/g)	74.6 ± 0.01	76.5 ± 0.1	77.0 ± 0.1	77.5 ± 0.5

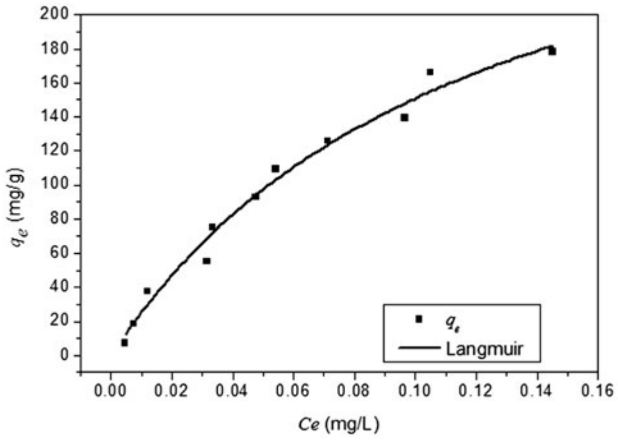

Fig. 7. Isotherm fitted to the Langmuir model.

Table 5
Isotherm constants for Cu(II) adsorption

Model	Constants		R^2
Langmuir	b (L/mg)	8.2 ± 1.6	0.98
	$q_{\max}$ (mg/g)	334 ± 39	
Freundlich	K_F (mg/g)	691 ± 89	0.97
	n	1.4 ± 0.1	

Table 6
Adsorption capacities after each adsorption–desorption cycle

	q_e (mg/g)		
Cycles	HCl	HNO_3	EDTA
0	178.6	178.6	178.6
1	89.5	91.8	19.8
2	17.1	14.0	14.8
3	7.1	3.2	14.2

3.6.6 Adsorption–desorption cycles

The adsorption capacities after each adsorption–desorption cycle (with pH solutions of 3) are show in Table 6.

The adsorption capacities decreased after each adsorption–desorption cycle. The decrease in the adsorption capacities could be attributed to the solubility of chitosan under these conditions as reported by Ngah et al. [8], they used HNO_3 and EDTA as regenerating agents for an adsorbent of this kind.

4. Conclusions

The adsorbent material was not resistant to acidic solutions of pH 1, this could be attributed to the incompatibility of EGDE with acid solutions and the material was stable at pH 4. The highest adsorption capacity of the material was at initial pH of 5. The pseudo-second-order model describes the adsorption kinetics better than the pseudo-first model. Experimental data were best fitted to the Langmuir isotherm, which involves the formation of a monolayer. The negative values of the Gibbs free energy indicate that the process is spontaneous, and the positive enthalpy indicates that the process is endothermic. These results indicate that material is a good potential adsorbent to remove Cu(II) from aqueous solutions.

Acknowledgements

The authors thank to the Tecnológico Nacional de México (project 4625.12-P) and CONACYT (project 131174Q) for the financial support and for the scholarship No. 34194 granted to N. F. A.

References

[1] P.R. Puranik, K.M. Paknikar, Biosorption of lead, cadmium, and zinc by citrobacter strain MCM B-181: Characterization studies, Biotechnol. Prog. 15 (1999) 228–237.

[2] S.T. Ramesh, R. Gandhimathi, P.V. Nidheesh, N. Badabhagni, K.S. Bharathi, Breakthrough data analysis of adsorption of Cd (II) on Coir pith column, Electron. J. Environ. Agric. Food Chem. 10 (2011) 2487–2505.

[3] T.C. Hsu, Experimental assessment of adsorption of Cu^{2+} and Ni^{2+} from aqueous solution by oyster shell powder, J. Hazard. Mater. 171 (2009) 995–1000.

[4] C.M. Futalan, C.C. Kan, M.L. Dalida, C. Pascua, M.W. Wan, Fixed-bed column studies on the removal of copper using chitosan immobilized on bentonite, Carbohydr. Polym. 83 (2011) 697–704.

[5] S. Hong, C. Wen, J. He, F. Gan, Y.S. Ho, Adsorption thermodynamics of Methylene Blue onto bentonite, J. Hazard. Mater. 167 (2009) 630–633.

[6] M. Al-Ghouti, M.A.M. Khraisheh, M.N.M. Ahmad, S. Allen, Thermodynamic behaviour and the effect of temperature on the removal of dyes from aqueous solution using modified diatomite: A kinetic study, J. Colloid Interface Sci. 287 (2005) 6–13.

[7] W. Kaminski, E. Tomczak, K. Jaros, Interactions of metal ions sorbed on chitosan beads, Desalination 218 (2008) 281–286.

[8] W.W. Ngah, A. Kamari, Y.J. Koay, Equilibrium and kinetics studies of adsorption of copper (II) on chitosan and chitosan/PVA beads, Int. J. Biol. Macromol. 34 (2004) 155–161.

[9] Y.S. Ho, G.A. McKay, Comparison of chemisorption kinetic models applied to pollutant removal on various sorbents, Process Saf. Environ. Prot. 76 (1998) 332–340.

[10] Y.S. Ho, G.A. McKay, Pseudo-second order model for sorption processes, Process Biochem. 34 (1999) 451–465.

[11] Y.S. Ho, Pseudo-isotherms using a second order kinetic expression constant, Adsorption 10 (2004) 151–158.

[12] Y.S. Ho, Isotherms for the sorption of lead onto peat: Comparison of linear and non-linear methods, Pol. J. Environ. Stud. 15 (2009) 81–86.

[13] Y.S. Ho, Review of second-order models for adsorption systems, J. Hazard. Mater. 136 (2006) 681–689.

[14] J. Wang, C. Chen, Biosorbents for heavy metals removal and their future, Biotechnol. Adv. 27 (2009) 195–226.

[15] S. Babel, T.A. Kurniawan, Low-cost adsorbents for heavy metals uptake from contaminated water: A review, J. Hazard. Mater. 97 (2003) 219–243.

[16] S.E. Bailey, T.J. Olin, R.M. Bricka, D.D. Adrian, A review of potentially low-cost sorbents for heavy metals, Water Res. 33 (1999) 2469–2479.

[17] W.W. Ngah, C.S. Endud, R. Mayanar, Removal of copper(II) ions from aqueous solution onto chitosan and cross-linked chitosan beads, React. Funct. Polym. 50 (2002) 181–190.

[18] M.N.R. Kumar, A review of chitin and chitosan applications, React. Funct. Polym. 46 (2000) 1–27.

[19] E. Guibal, Interactions of metal ions with chitosan-based sorbents: A review, Sep. Purif. Technol. 38 (2004) 43–74.

[20] F. Zhao, B. Yu, Z. Yue, T. Wang, X. Wen, Z. Liu, C. Zhao, Preparation of porous chitosan gel beads for copper(II) ion adsorption, J. Hazard. Mater. 147 (2007) 67–73.

[21] W.W. Ngah, L.C. Teong, M.A.K.M. Hanafiah, Adsorption of dyes and heavy metal ions by chitosan composites: A review, Carbohydr. Polym. 83 (2011) 1446–1456.

[22] A. Kamari, W.W. Ngah, Isotherm, kinetic and thermodynamic studies of lead and copper uptake by H_2SO_4 modified chitosan, Colloids Surf. B: Biointerfaces 73 (2009) 257–266.

[23] A.H. Chen, S.C. Liu, C.Y. Chen, Comparative adsorption of Cu(II), Zn(II), and Pb(II) ions in aqueous solution on the crosslinked chitosan with epichlorohydrin, J. Hazard. Mater. 154 (2008) 184–191.

[24] K.A. Hernández-Hernández, M. Solache-Ríos, M.C. Díaz-Nava, Removal of brilliant blue FCF from aqueous solutions using an unmodified and iron-modified bentonite and the thermodynamic parameters of the process, Water Air Soil Pollut. 224 (2013) 1–11.

[25] H.H. Huang, L.G. Twidwell, C.A. Young, in: D.G. Dixon (Eds), Proceedings of the International Symposium on Computational Analysis in Hydrometallurgy, Canadian Institute of Mining, Metallurgy and Petroleum, Calgary, Canada, 2005.

[26] A.M. Cardenas-Peña, J.G. Ibanez, R. Vasquez-Medrano, Determination of the point of zero charge for electrocoagulation precipitates from an iron anode, Int. J. Electrochem. Sci. 7 (2012) 6142–6153.

[27] M. Kacuráková, P. Capek, V. Sasinkova, N. Wellner, A. Ebringerova, FT-IR study of plant cell wall model compounds: Pectic polysaccharides and hemicelluloses, Carbohydr. Polym. 43 (2000) 195–203.

[28] W.L. Du, S.S. Niu, Z.R. Xu, Y.L. Xu, Preparation, characterization, and adsorption properties of chitosan microspheres crosslinked by formaldehyde for copper (II) from aqueous solution, J. Appl. Polym. Sci. 111 (2009) 2881–2885.

[29] M.R. Gandhi, G.N. Kousalya, N. Viswanathan, S. Meenakshi, Sorption behaviour of copper on chemically modified chitosan beads from aqueous solution, Carbohydr. Polym. 83 (2011) 1082–1087.

[30] Z. Cheng, X. Liu, M. Han, W. Ma, Adsorption kinetic character of copper ions onto a modified chitosan transparent thin membrane from aqueous solution, J. Hazard. Mater. 182 (2010) 408–415.

[31] A. Ghaee, M. Shariaty-Niassar, J. Barzin, T. Matsuura, Effects of chitosan membrane morphology on copper ion adsorption, Chem. Eng. J. 165 (2010) 46–55.

[32] J. He, Y. Lu, G. Luo, Ca(II) imprinted chitosan microspheres: An effective and green adsorbent for the removal of Cu(II), Cd(II) and Pb(II) from aqueous solutions, Chem. Eng. J. 244 (2014) 202–208.

[33] M.L.P. Dalida, A.F.V. Mariano, C.M. Futalan, C.C. Kan, W.C. Tsai, M.W. Wan, Adsorptive removal of Cu(II) from aqueous solutions using non-crosslinked and crosslinked chitosan-coated bentonite beads, Desalination 275 (2011) 154–159.

[34] C.P. Wang, B.L. Wang, J.T. Liu, Li Yu, H.W. Sun, J.Z. Wu, Adsorption of Cd(II) from acidic aqueous solutions by tourmaline as a novel material, Chin. Sci. Bull. 57 (2012) 3218–3225.

[35] B. Volesky, Z.R. Holan, Biosorption of heavy metals, Biotechnol. Prog. 11 (1995) 235–250.